Battery State-of-Charge and Parameter Estimation Algorithm Based on Kalman Filter

Dragicevic, Tomislav; Sucic, Stjepan; Guerrero, Josep M.

Published in:
Proceedings of the 2013 IEEE EUROCON

DOI (link to publication from Publisher):
10.1109/EUROCON.2013.6625179

Publication date:
2013

Document Version
Early version, also known as pre-print

This is the preprint version of the paper T. Dragicevic, S. Sucic, J. M. Guerrero "Battery state-of-charge and parameter estimation algorithm baed on Kalman filter," Proc. on IEEE EUROCON 2013, pp. 1519-1524.

Battery State-of-Charge and Parameter Estimation Algorithm Based on Kalman Filter

Tomislav Dragicevic [#1], Stjepan Sucic [*2], Josep M. Guerrero [#3]

[#] *Department of Energy Technology, Aalborg University*
Pontoppidanstraede 101, 9220 Aalborg, Denmark
[1] tdr@et.aau.dk
[3] joz@et.aau.dk

[*] *Koncar KET*
Fallerovo setaliste 22, 10000 Zagreb, Croatia
[2] stjepan.sucic@koncar-ket.hr

***Abstract*—Electrochemical battery is the most widely used energy storage technology, finding its application in various devices ranging from low power consumer electronics to utility back-up power. All types of batteries show highly non-linear behaviour in terms of dependence of internal parameters on operating conditions, momentary replenishment and a number of past charge/discharge cycles. A good indicator for the quality of overall customer service in any battery based application is the availability and reliability of these informations, as they point out important runtime variables such as the actual state of charge (SOC) and state of health (SOH). Therefore, a modern battery management systems (BMSs) should incorporate functions that accommodate real time tracking of these non-linearities. For that purpose, Kalman filter based algorithms emerged as a convenient solution due to their ability to adapt the underlying battery model on-line according to internal processes and measurements. This paper proposes an enhancement of previously proposed algorithms for estimation of the battery SOC and internal parameters. The validity of the algorithm is confirmed through the simulation on experimental data captured from the lead acid battery stack installed in the real-world remote telecommunication station.**

***Index Terms*—Lead acid battery, Kalman filter, estimation, state-of-charge, battery management system.**

I. Introduction

Secondary (rechargeable) batteries are widely used in applications such as starting, lighting and ignition (SLI), consumer electronic devices, vehicles and emergency and standby power supplies. Due to relatively low price and descent characteristics, the most prevalent technology for today's stationary applications is lead-acid, accounting for 69% share of the worldwide market [1]. As the lifetime of this battery is sensitive to overcharge and deep discharge, over- and under-voltage circuits were commonly used for protection purposes in the past [2]. However, with an expansion of control capabilities in power electronics, multiplex battery managements systems (BMSs) started to replace former circuits in many applications.

One of the most important tasks within the typical BMS is a reliable real time determination of the state-of charge (SOC) [3], [4]. SOC is essentially a ratio between the instantaneous energy that can be depleted out of battery and maximum energy that can be stored in it. This operational parameter can not be directly measured and its assessment relies exclusively on estimation. An accurate estimate facilitates efficient and safe operation of the battery by disabling under- and over-charge conditions.

A good overview and comparative analysis of several different direct and indirect methods for SOC estimation have been performed in [5]. The indirect strategies are related to specific measurements of SOC related parameters such as the specific gravity (only for lead-acid batteries) and internal resistance. The first one is a convenient way for estimating the SOC during the discharge process but is somewhat unreliable during charging as the there is a lag associated with incomplete mixing of the electrolyte at moderate battery voltages. On the other hand, the impedance spectroscopy method was found to be more relevant for SOH estimation as internal resistance is its most important indicator [6]. Moreover, both kinds of these measurements were found to be quite expensive and impractical to implement.

The ampere- or coulomb-counting method, which is based on the capacity-scaled integration of the battery current is the most widely used on-line direct strategy. However, it is prone to several runtime errors related to complete dependence of the method on the accuracy of current measurement and to difficulty of on-line assessment of the actual battery capacity. Also, without an accurate initial SOC, it has no chance for later correction of the estimate [7]. Thus, in order to achieve more resilience against the measurement uncertainty, a model of the particular battery stack, such as the one presented in [8], can be used for the battery open-circuit voltage (OCV) estimation, from which the actual SOC can be utterly extracted given that the SOC vs. OCV relationship is known. However, knowing that the parameters of the battery model are even in the best case extracted to a limited range of operating conditions and that they are changing with the cycle life, it is intuitively clear that this approach may give false results without regular calibration.

On the other hand, real time estimation of the parameters and states within the battery model that are otherwise difficult to measure emerged as a potential resolution to aforementioned problems. To that end, application of the Kalman filter,

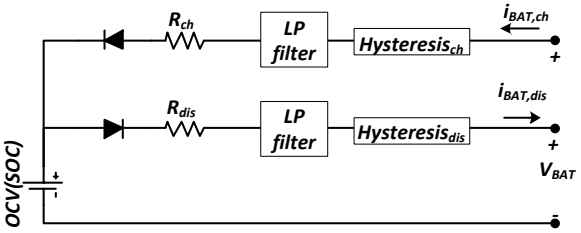

Fig. 1. Battery model utilized in Kalman filter.

a minimum mean-square estimator, started to gain considerable attention for the battery SOC and state-of-health (SOH) estimations [9]–[11]. Its specificity is that it optimally estimates the states of the dynamical system described by state flow equations and measurements that are prone to noise.

The basic version of the algorithm operates in a two-step process:

- Prediction step - The expected output is generated based on the underlying model where the model inputs and previous values of the internal model states are accounted.
- Correction step - The calculated output of the model is compared with output measurements and state estimates are accordingly updated so as to reduce the difference. Given that there is a number of states in the model, every respective state estimate is updated using its associated weight. The weight of some state estimate determines its degree of certainty. So, the higher the weight, the estimate is considered less accurate it is enforced to change more in the correction step.

The variation of this kind of an algorithm was applied in this paper as well. The paper is organized as follows. Section II describes the battery model which is used in the Kalman filter. Section III presents the conventional dual Kalman filter for SOC and parameter estimation. Section IV gives the proposal of estimation enhancement, while the experimental results are reported in Section V. Finally, Section VI draws the conclusion.

II. Battery Model

The first prerequisite for the practical implementation of the Kalman filter is the existence of a convenient battery model. Here, the model similar to the one developed in [12] is utilized. However, in the order to distinguish the charge and discharge parameters, two separate circuits have been used. Moreover, due to discrete nature of the Kalman filter, the differential equations that represent the battery dynamics have been replaced with the difference equations. The battery model is shown in Fig. 1, and the features of its constituent parts are explained below. The SOC is calculated according to the ampere-counting method as

$$SOC_{k+1} = SOC_k - \eta \frac{i_{BAT,k}}{C_{BAT}} \Delta t, \tag{1}$$

where SOC_k is SOC in the previous time step, η is charging/discharging efficiency, $i_{BAT,k}$ is the battery current, C_{BAT} is the battery nominal capacity and Δt is a discrete time step. Then, for every SOC, OCV of the 24 lead acid cell battery stack is calculated with a linear function OCV(SOC) which was extracted in the earlier work performed by the author [13]:

$$OCV(SOC_k) = 0.035582 \cdot SOC_k + 47.698. \tag{2}$$

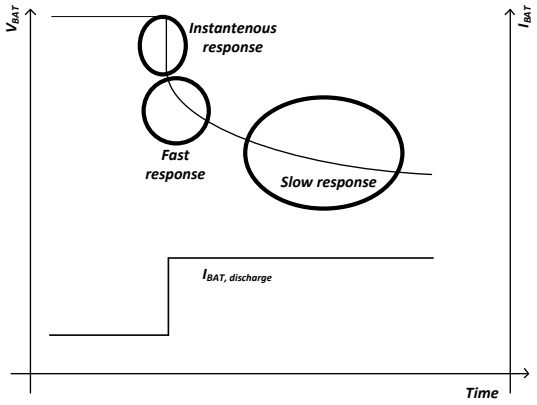

Fig. 2. Typical battery terminal voltage response to a current step.

The instantaneous voltage drop is accounted with separate charge and discharge resistances, R_{ch} and R_{dis}, whereas the transient voltage drop is modelled with a combination of the first order low pass filter (fast dynamics) and a hysteresis effect (slow dynamics). The discrete filter can be expressed with the following state-space representation:

$$\begin{cases} filt(i_{BAT,k}) = C_f f_k \\ f_{k+1} = A_f f_k + B_f i_{BAT,k}. \end{cases} \tag{3}$$

where A_f, B_f and C_f are the filter state transition matrix, state input matrix and state output matrix respectively. The slow dynamics are modelled with the difference equation in which the parameter γ points the response speed, while A_{hist} gives the hysteresis amplitude:

$$h_{k+1} = exp\left(-\left|\frac{\eta \cdot i_{BAT,k} \cdot \gamma \cdot \Delta t}{C_{BAT}}\right|\right) + \left(1 - exp\left(-\left|\frac{\eta \cdot i_{BAT,k} \cdot \gamma \cdot \Delta t}{C_{BAT}}\right|\right)\right) A_{hist}. \tag{4}$$

The sum of all aforementioned responses gives the battery terminal voltage which is compared to the actual voltage measurement in the correction step:

$$y_k = OCV(SOC_k) + h_k + filt(i_{BAT,k}) - Ri_{BAT,k}. \tag{5}$$

With (5), a typical battery terminal voltage response to a current step (see. Fig. 2) can be perfectly matched, given that the selection of associated parameters is correct.

The next step is to show how the features of the Kalman filter can be exploited in order to accomplish the self tuning

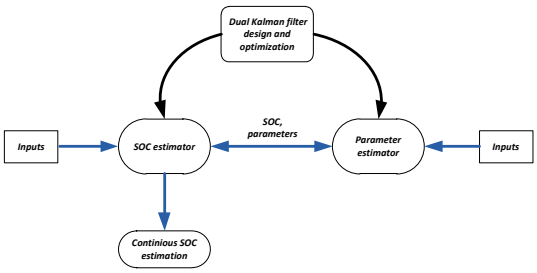

Fig. 3. Development process of the dual extended Kalman filter.

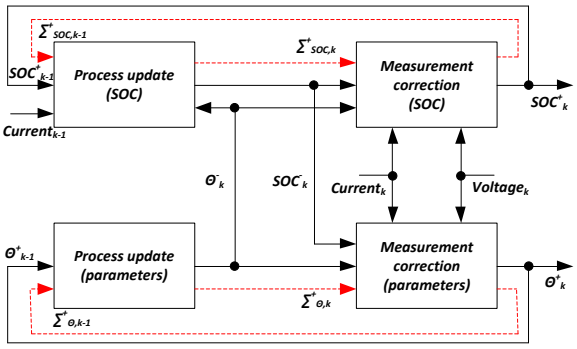

Fig. 4. Block diagram of the dual extended Kalman filter. Here, the black lines represent the flow of parameters and SOC estimates, while the red lines represent covariances.

capability of SOC and the other parameters in presented model.

III. Kalman Filter

As already stated before, the parameters of the model vary with changes in operating conditions and with the life-cycle of the battery. Therefore, for obtaining the correct estimate of SOC, also the estimates of underlying model parameters should be accurate. To that end, Plett has developed a Kalman filter based simultaneous state and parameter estimation concept in a series of three papers [14]–[16]. In his work, he split the state and parameter estimation time-line into two frames, where SOC was the representative of the rapidly changing frame, while the parameters such as internal resistances and hysteresis comprised the slowly varying frame [1]. The algorithm was embedded in two separate sections in order to maintain a limited dimensions of associated state-transition matrices, with each one of them accommodating one frame. The basic flowchart of the algorithm is shown in Fig. 3, where black arrows indicate the off-line design process, while the blue arrows indicate the states and parameters flow during the on-line operation.

The basic principle of operation is to calculate a new SOC in every time step with the equation (1) and then to adapt it according to (5), using the momentary estimates. Finally, the slowly varying parameters are updated as well using the previous estimate of SOC, as they would remain constant if new SOC estimate is used.

A detailed overview of the process flow within the dual Kalman filter is shown in Fig. 4, while the underlying calculation is depicted in the set of equations from (7) to (21). One can note that the subscript $-$ in the set of equations indicates the value of the estimate during an intermediate step, while the subscript $+$ indicates its the final value. These equations can be linked with the battery model shown in Fig. 1. So, the momentary SOC estimate is contained in the x_k variable. The parameter vector is Θ, and it contains the current estimates of internal resistances, the hysteresis amplitude and the hysteresis time constant:

$$\Theta = [R_{ch}\, R_{dis}\, A_{hist}\, \gamma]. \tag{6}$$

[1]The meaning of the term *frame* is related to the speed of parameter adaptation.

The function that incorporates the coulomb counting is $f(x_k, u_k, \Theta_k)$, while $g(x_k, u_k, \Theta_k)$ calculates the battery terminal voltage according to (5). The variable u_k comprises the battery current $i_{BAT,k}$. Apart from propagation of the estimates, also the associated covariances, Σ_{x_k} and Σ_{Θ_k}, are updated in every time step. They are used for calculation of the respective Kalman gain matrices, shown in equations (16) and (19) respectively.

A step by step evaluation of the procedure is as follows. Given the initial values of SOC and other model parameters, represented in (10) and (11), the parameter transition was chosen as the first step (see equation (12)). There, the regular time update was omitted due to in-existence of predictable variations of the parameters. So, in order to accommodate the slow parameter variation, only the parameter uncertainty was included by adding a covariance matrix Σ_r, which is driven by the independent noise r_k. This step is followed by the SOC time-transition step, shown in (14), and associated calculation of the SOC covariance from (15). In this case, apart from adding the associated covariance matrix Σ_ω, the overall covariance calculation also includes the algebra with the state transition matrix A_{k-1}.

The last two steps, termed as states and parameters measurement updates, comprise the actual adaptation of the parameters. In these steps, first the corresponding Kalman gains are computed and then they are used for the adaptation of SOC and other parameters in order to decrease the error between the measurement of the battery terminal voltage and the output of the battery model.

The duality of Kalman filter implies a careful integration of the equations from both frames into a single filter. The order of execution of equations arising from both frames must be set so that the adaptation of SOC and parameters takes place without mutual infighting. As both adaptations occur on a principle of tuning the model according to the measured output, change of SOC in one way may induce the change of parameters to the other way, if designed incorrectly. Therefore, the correction step of SOC was given a priority over parameter correction. Moreover, in order to further decouple the dual tuning procedure, the adaptation of parameters was set to take

place using the calculation with the SOC estimate from the previous step.

SUMMARY OF THE DUAL KALMAN FILTER

Process description:

$$x_{k+1} = f(x_k, u_k, \Theta_k) + \omega_k,\ \Theta_{k+1} = \Theta_k + r_k \quad (7)$$

and

$$y_k = g(x_k, u_k, \Theta_k) + v_k,\ d_k = g(x_k, u_k, \Theta_k) + e_k \quad (8)$$

The state matrices are obtained via linearisation :

$$A_{k-1} = \frac{\partial f(x_{k-1}, u_{k-1}, \Theta_k^-)}{\partial x_{k-1}},\ C_k^x = \frac{\partial g(x_k, u_k, \Theta_k^-)}{\partial x_k},$$

$$C_k^\Theta = \frac{\partial g(x_k^-, u_k, \Theta)}{\partial \Theta} \quad (9)$$

Initialization:

$$\Theta_0^+ = \mathrm{E}(\Theta_0),\ \Sigma_{\Theta_0^+} = \mathrm{E}[(\Theta_0 - \Theta_0^+)(\Theta_0 - \Theta_0^+)^T] \quad (10)$$

$$x_0^+ = \mathrm{E}(x_0),\ \Sigma_{x_0^+} = \mathrm{E}[(x_0 - x_0^+)(x_0 - x_0^+)^T] \quad (11)$$

Calculation procedure:

P1: Parameters time update

$$\Theta_k^- = \Theta_{k-1}^+ \quad (12)$$

$$\Sigma_{\Theta_k^-} = \Sigma_{\Theta_{k-1}^+} + \Sigma_r \quad (13)$$

S1: State time update

$$x_k^- = f(x_{k-1}^-, u_{k-1}, \Theta_k^-) \quad (14)$$

$$\Sigma_{x_k^-} = A_{k-1}\Sigma_{x_{k-1}^+}A_{k-1}^T + \Sigma_\omega \quad (15)$$

S2: State measurement update

$$L_k^x = \Sigma_{x,k}^-(C_k^x)^T[C_k^x\Sigma_{x,k}^-(C_k^x)^T + \Sigma_v]^{-1} \quad (16)$$

$$x_k^+ = x_k^- + L_k^x[y_k - g(x_k^-, u_k, \Theta_k^-)] \quad (17)$$

$$\Sigma_{x,k}^+ = (I - L_k^x C_k^x)\Sigma_{x,k}^- \quad (18)$$

P2: Parameters measurement update

$$L_k^\Theta = \Sigma_{\Theta,k}^-(C_k^\Theta)^T[C_k^\Theta\Sigma_{\Theta,k}^-(C_k^\Theta)^T + \Sigma_e]^{-1} \quad (19)$$

$$\Theta_k^+ = \Theta_k^- + L_k^\Theta[y_k - g(x_k^-, u_k, \Theta_k^-)] \quad (20)$$

$$\Sigma_{\Theta,k}^+ = (I - L_k^\Theta C_k^\Theta)\Sigma_{\Theta,k}^- \quad (21)$$

After the representation of equations of the dual Kalman filter, one should note that this Kalman filter should incorporate the term *Extended* as the model of the system which is tracked is non-linear due to transient hysteresis term. Therefore, as the Kalman filter in this form implies linear state transitions, some of the equations must be linearised, as shown in (9). Having in mind that the linearisation of the first and second term is straightforward (The function $f(x_k, u_k, \Theta_k)$ essentially describes the coulomb counting and its derivative over SOC is equal to unity. On the other hand, the function $g(x_k, u_k, \Theta_k)$ describes the battery terminal voltage. As the only variable

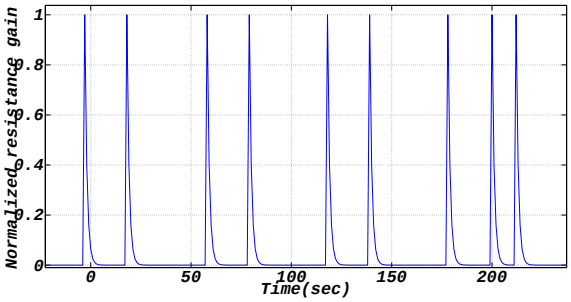

Fig. 5. Illustration of rapid changes in battery charging current that impact the internal resistance term (This excerpt correspond to around 8h and 45 minutes from Fig. 7).

dependant on SOC is OCV, having a linear dependence, the associated derivative is constant and indicates the slope of the OCV vs. SOC curve), only the derivative of $g(x_k, u_k, \Theta_k)$ along the Θ requires somewhat tedious algebra:

$$\frac{dg(x_k, u_k, \Theta)}{d\Theta} = \frac{\partial g(x_k, u_k, \Theta)}{\partial \Theta} + \frac{\partial g(x_k, u_k, \Theta)}{\partial x_k}\frac{dx_k}{d\Theta}, \quad (22)$$

where the derivation of g along x_k is always equal to unity while

$$\frac{\partial g(x_k, u_k, \Theta)}{\partial \Theta} = [-i_{charge}\ -i_{discharge}\ 0\ 0] \quad (23)$$

and

$$\frac{dx_k}{d\Theta} = \frac{\partial f(x_{k-1}, u_{k-1}, \Theta)}{\partial \Theta} + \frac{\partial f(x_{k-1}, u_{k-1}, \Theta)}{\partial x_{k-1}}\frac{dx_{k-1}}{d\Theta}. \quad (24)$$

If the term $exp\left(-\left|\frac{\eta \cdot i_{BAT,k} \cdot \gamma \cdot \Delta t}{C_{BAT}}\right|\right)$ from (4) is replaced with Fi_k, the partial derivative of f along the parameter vector Θ may be expressed as follows:

$$\frac{\partial f(x_{k-1}, u_{k-1}, \Theta)}{\partial \Theta} = \left[0\ 0\ (1 - Fi_{k-1})\ (A_{hist} - h_{k-i})\left|\frac{\eta \cdot i_{BAT,k}\Delta t}{C_{BAT}}\right| Fi_{k-1}\right]. \quad (25)$$

The final part of the derivative term may be obtained by calculating

$$\frac{\partial f(x_k, u_k, \Theta)}{\partial x_{k-1}}\frac{dx_{k-1}}{d\Theta} = F_{k-1}\frac{dx_{k-1}}{d\Theta}. \quad (26)$$

IV. ENHANCEMENT OF THE INTERNAL RESISTANCE ESTIMATION

The process described in the previous section implies the use of covariances which are calculated according to the actual system conditions. So, the first two columns of vector C_k^Θ contain the momentary charge and discharge currents. This vector is then included into the formula (19), where the corresponding Kalman gain vector is calculated. The values of respective elements within this vector actually determine the extent to which each of the elements in Θ_k^- is altered when the correction step of (20) is applied. If the covariance

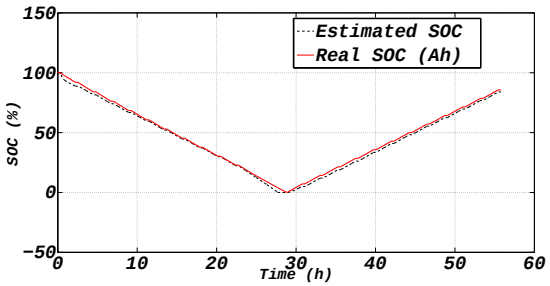

Fig. 6. Application of developed Kalman filter to the discharge and charge tests presented in [13].

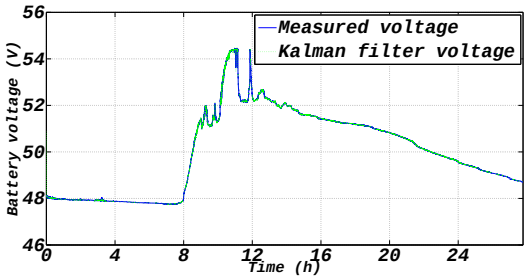

Fig. 7. Comparison of measured voltage response and the output of dual extended Kalman filter with performance enhancer.

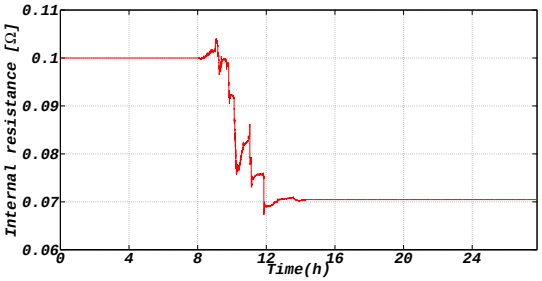

Fig. 8. Self-tuning of the battery internal discharging resistance.

calculation is left to the natural evolution of the algorithm, an external influence on the propagation of parameter values is not possible. In this case, they are altered automatically, without respect to battery conditions in which the terminal voltage changes may depend predominantly on a certain set of parameters. Therefore, the enhancement of the dual Kalman filter is related with application of external tuning of corresponding elements within the C_k^{Θ} vector.

More specifically, in order to make use of the knowledge related to dynamic battery behaviour in pulsed current conditions, the automatic self-tuning of the elements associated with internal resistances within the parameter Kalman gain vector is proposed. To that end, one may recall the typical shape of the battery terminal voltage transient which follows the current step. As recalled from Fig. 2, it consists of an instantaneous voltage drop and a transient voltage term that can be considered to consist of a number of exponential terms with different time constants. In this case, the theoretical transient voltage is designed to consist of three different terms; i.e. the instantaneous term, the fast transient and a slow transient. First two of them are accommodated by the internal resistance and discrete low pass filter respectively, while the latter is based on the hysteresis effect described by equation (4).

The proposed enhancement is based on the exploitation of the fact that instantaneous voltage change followed by the battery current step change depends exclusively on internal resistance. So, if the step occurs during the charging period, momentarily voltage drop is associated with R_{ch}, and with R_{dis} if it occurs during the discharging. To that end, unlike having the charging and discharging current as the first two elements in C_k^{Θ} vector, these elements are artificially increased once the pulse currents are detected. This feature is achieved by the application of a linear discrete filter that has the same structure such as the one used for emulating fast voltage transients (see (3)). However, here it is used for instantaneous increase of the corresponding element in the C_k^{Θ} vector so as to increase the associated Kalman gain as well. As the filter was tuned to have a zero dc gain, its response decays exponentially with the time that follow the initial current step. In order to perform the enhancement, the first two elements of equation (23) were reformulated as follows:

$$\begin{cases} abs\left(sign(i_{charge})\right) + 5 \cdot ft_{ch} \\ -abs\left(sign(i_{discharge})\right) - 5 \cdot ft_{dis} \end{cases} \tag{27}$$

where ft_{ch} and ft_{dis} were calculated as:

$$\begin{cases} ft_{ch,k} = 0.4 ft_{ch,k} + abs(i_{BATch,k} - i_{BATch,k-1}) > 0.5 \\ ft_{dis,k} = 0.4 ft_{dis,k} + abs(i_{BATdis,k} - i_{BATdis,k-1}) > 0.5. \end{cases} \tag{28}$$

An example of rapid changes (with amplitude more than 0.5 A) of the battery charging current and its impact on the first element in C_k^{Θ} vector is shown in Fig. 5. This result came as the validation of the Kalman filter on experimental battery measurements in a real industrial environment. The rest of results are presented in the next section.

V. Simulation Results

First, the version of the dual extended Kalman filter without the proposed enhancement has been implemented in the lab and was tested on the previously experimentally recorded discharge and charge voltage curves (see [13]).

The corresponding tracking of the SOC is shown in Fig. 6. A good behaviour of the algorithm can be explained by the relatively static environment in which the test has been performed. Thus, the limited variation of the parameters allows for an accurate SOC estimation even, as the covariance matrices are kept at a relatively low value.

On the other hand, the Kalman filter expanded with an internal resistance enhancer was tested on the battery data recorded in the real remote telecommunication station. The station is

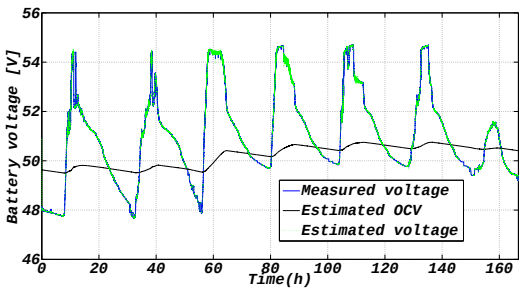

Fig. 9. Representation of the long term tracking of the battery stack terminal voltage realized by means of enhanced Kalman filter.

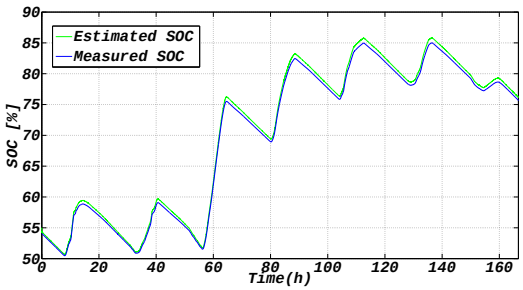

Fig. 10. Representation of the long term tracking of the battery stack SOC realized by means of enhanced Kalman filter.

supplied exclusively by RESs, i.e. two wind turbines and a PV array. Therefore, the environment in which the battery operates was rather turbulent from electrical point of view. There, the frequent current steps were caused by the combined effect of wind gusts, PV array cloud shadowing and a non-constant load profile. Developed filter applied to a single day of experimental data showed a very good measurement tracking, as shown in Fig. 7. The algorithm was tracking the instantaneous changes in the total battery current and produced the corresponding changes in the internal resistance covariation matrix. So, every time when the current change within one second surpassed the value of 0.5 A, the instantaneous rise of the gain followed by its exponential decay appeared in the respective matrix, causing the faster convergence of the instantaneous charging resistance value. see Fig. The effect is specifically accentuated during the 8th and 12th hour, as seen in Fig. 8.

The filter was also tested on a larger time horizon, which was more indicative for the correctness of the SOC estimation. So, the estimate of the battery terminal voltage and battery OCV during one week of the operation is shown in Fig. 9, while the corresponding evolution of SOC is shown in Fig. 10.

VI. Conclusion

This paper was focused on the development of reliable SOC and battery parameter estimation algorithm. For that purpose, a dual extended Kalman filter has been selected due to possibility of obtaining very precise tracking with measurements of only electrical quantities. The algorithm was embedded in Matlab and was tested on previously performed experimental tests, showing a good tracking given that the initial conditions for parameters were set close to the actual ones. However, the selection of the gain in the state transition matrix for the internal resistance estimation proved to be difficult due to overlap with the hysteresis parameter. On the other hand, once subjected to a turbulent environment of the RES based remote telecommunication facility, the rapidly changing battery current was used as the trigger to increase the respective gains in the parameter covariance matrix. In this way, it was ensured that internal resistances always converge to correct values following any significant current step.

References

[1] D. Linden and T. B. Reddy, *Handbook of Batteries*. McGraw-Hill, 2002.

[2] J. Cao and A. Emadi, "Batteries need electronics," *Industrial Electronics Magazine, IEEE*, vol. 5, pp. 27 –35, march 2011.

[3] J. Chatzakis, K. Kalaitzakis, N. Voulgaris, and S. Manias, "Designing a new generalized battery management system," *Industrial Electronics, IEEE Transactions on*, vol. 50, pp. 990 – 999, oct. 2003.

[4] S. Vazquez, S. Lukic, E. Galvan, L. Franquelo, and J. Carrasco, "Energy storage systems for transport and grid applications," *Industrial Electronics, IEEE Transactions on*, vol. 57, pp. 3881 –3895, dec. 2010.

[5] S. Piller, M. Perrin, and A. Jossen, "Methods for state-of-charge determination and their applications," *Journal of Power Sources*, vol. 96, no. 1, pp. 113 – 120, 2001. Proceedings of the 22nd International Power Sources Symposium.

[6] F. Huet, "A review of impedance measurements for determination of the state-of-charge or state-of-health of secondary batteries," *Journal of Power Sources*, vol. 70, no. 1, pp. 59 – 69, 1998.

[7] K. Kutluay, Y. Cadirci, Y. Ozkazanc, and I. Cadirci, "A new online state-of-charge estimation and monitoring system for sealed lead-acid batteries in telecommunication power supplies," *Industrial Electronics, IEEE Transactions on*, vol. 52, pp. 1315 – 1327, oct. 2005.

[8] M. Ceraolo, "New dynamical models of lead-acid batteries," *Power Systems, IEEE Transactions on*, vol. 15, pp. 1184 –1190, nov 2000.

[9] B. Bhangu, P. Bentley, D. Stone, and C. Bingham, "Nonlinear observers for predicting state-of-charge and state-of-health of lead-acid batteries for hybrid-electric vehicles," *Vehicular Technology, IEEE Transactions on*, vol. 54, pp. 783 – 794, may 2005.

[10] A. Vasebi, S. Bathaee, and M. Partovibakhsh, "Predicting state of charge of lead-acid batteries for hybrid electric vehicles by extended kalman filter," *Energy Conversion and Management*, vol. 49, no. 1, pp. 75 – 82, 2008.

[11] M. Charkhgard and M. Farrokhi, "State-of-charge estimation for lithium-ion batteries using neural networks and ekf," *Industrial Electronics, IEEE Transactions on*, vol. 57, pp. 4178 –4187, dec. 2010.

[12] M. Chen and G. Rincon-Mora, "Accurate Electrical Battery Model Capable of Predicting Runtime and IV Performance," *IEEE Transactions on Energy Conversion*, vol. 21, pp. 504–511, June 2006.

[13] T. Dragicevic, T. Capuder, M. Jelavic, and D. Skrlec, "Modelling and Simulation of Isolated DC Microgrids Supplied by Renewable Energy Resources, volume = 1," in *2011, Conference on Sustainable Development of Energy, Water and Environment Systems*.

[14] G. L. Plett, "Sigma-point kalman filtering for battery management systems of lipb-based hev battery packs: Part 1: Introduction and state estimation," *Journal of Power Sources*, vol. 161, no. 2, pp. 1356 – 1368, 2006.

[15] G. L. Plett, "Sigma-point kalman filtering for battery management systems of lipb-based hev battery packs: Part 2: Simultaneous state and parameter estimation," *Journal of Power Sources*, vol. 161, no. 2, pp. 1369 – 1384, 2006.

[16] G. L. Plett, "Extended kalman filtering for battery management systems of lipb-based hev battery packs: Part 3. state and parameter estimation," *Journal of Power Sources*, vol. 134, no. 2, pp. 277 – 292, 2004.